

CHARGED PARTICLE CORRELATIONS IN
200 AND 300 GeV/c pp INTERACTIONS*,**

Argonne National Laboratory
Iowa State University
University of Maryland
Michigan State University
National Accelerator Laboratory

ABSTRACT

Two particle correlation functions have been studied in terms of C.M. rapidity and C.M. and laboratory pseudorapidity variables. The data presented here, obtained with the NAL 30-inch bubble chamber-wide gap spark chamber hybrid system, together with previously published ISR data indicate that the rapidity density function evaluated in the central region, $R(0,0)$, is essentially the same in terms of all variables studied and is energy independent.

*Work supported in part by the U.S. Atomic Energy Commission and the National Science Foundation.

**Paper submitted to the XVII International Conference on High Energy Physics, London, England, 1-10 July, 1974 by G. A. Smith on behalf of the collaboration.

The existence of strong two-particle correlations at ISR and NAL energies has been well established. The ISR experiments have measured $R(0,0) \approx 0.6-0.7$, where R is the rapidity density function expressed in terms of pseudorapidity (η) variables, between charged particles¹ as well as between charged particles and gamma-rays². Measured in terms of the rapidity (y) variable, NAL experiments^{3,4,5} have measured $R(0,0) \approx 0.6$ for all charged particles and $R(0,0) \approx 0.4$ for negative particles only.

In this paper we study the possible effects of different variables on the R functions, using data from pp collisions at 200 and 300 GeV/c obtained with the 30-inch bubble chamber-wide gap chamber hybrid system⁶. Forward tracks in the laboratory within an angle of $\pm 4^\circ$ have been detected in the downstream spark chambers, resulting in substantially more precise angle and momentum measurements for those tracks. The variables we consider are (1) the C.M. rapidity, y_{CM} ; (2) the C.M. pseudorapidity η_{CM} ; and (3) the laboratory pseudorapidity, η_{LAB} , where in the latter case 3.2(3.5) has been subtracted at 200 GeV/c (300 GeV/c) for ease of comparison with C.M. variables. The single particle density functions

$$\rho = (d\sigma/dy_{CM})/\sigma_{inel}, (d\sigma/d\eta_{CM})/\sigma_{inel} \text{ and } d\sigma/d\eta_{LAB}/\sigma_{inel} \quad (1)$$

of the negative particles are shown in Figure 1. It is apparent from Figure 1 that in the region $|y|$ or $|\eta| < 1.0$ the choice of variable is important, witnessed by the substantial differences between the density functions.

The two particle correlation function,

$$R = \rho_{12} / \rho_1 \rho_2^{-1} \quad (2)$$

where

$$\rho_{12} = \left(\frac{d^2\sigma}{dy_{CM}(1) dy_{CM}(2)} \right) / \sigma_{inel}, \text{ etc.} \quad (3)$$

is shown in Figure 2. We note that, unlike the single particle spectra, the magnitude of $R(0,0) \approx 0.4$ remains constant, independent of the variables, both at 200 and 300 GeV/c. The detailed shapes of the R functions, however, depend on the variables used.

In Figure 3, we show the R functions for all charged particles and negative particles only at 200 GeV/c, from which we determine

$$R_{CC}(0,0) \approx 0.6 \quad (4)$$

and $R_{--}(0,0) \approx 0.4, \quad (5)$

in agreement with the previous determinations of these quantities in terms of rapidity variables.^{3,4,5}

These NAL data, together with the earlier ISR results, indicate that most probably $R(0,0)$ is independent of energy and choice of variables.

FIGURE CAPTIONS

Figure 1 - Single particle density functions $\rho \equiv \frac{d\sigma}{dy_{CM}} / \sigma_{inel}$,

$\frac{d\sigma}{dn_{CM}} / \sigma_{inel}$ and $\frac{d\sigma}{dn_{LAB}} / \sigma_{inel}$, for negative particles produced in pp interactions at 200 and 300 GeV/c.

Figure 2 - Rapidity density function $R = \frac{\rho_{12}}{\rho_1 \rho_2} - 1$ for the three variables for negative tracks produced in pp interactions at 200 and 300 GeV/c.

Figure 3 - Rapidity density function $R = \frac{\rho_{12}}{\rho_1 \rho_2} - 1$ for the η_{LAB} variable for charged-charged and negative-negative particle pairs.

REFERENCES AND FOOTNOTES

1. S. R. Amendolia, et al., Phys. Letters 48B, 359 (1974).
2. H. Dibon, et al., Phys. Letters 44B, 313 (1973).
3. "Inclusive Spectra of Secondaries From 200 GeV/c Proton-Proton Interactions Detected in the NAL 30-Inch Bubble Chamber-Wide Gap Spark Chamber Hybrid System", paper submitted to the 1973 Berkeley meeting of the Division of Particles and Fields, American Physical Society, Berkeley, California.
4. C.M. Bromberg, et al., Phys. Rev. D9, 1864 (1974).
5. R. Singer, et al., ANL/HEP 7368 (1974).
6. G. A. Smith, "The NAL 30-Inch Bubble Chamber-Wide Gap Spark Chamber Hybrid System". Proceedings of the 1973 Berkeley Meeting of the Division of Particles and Fields, American Physical Society, Berkeley, California, p. 500, and paper submitted to this conference.

pp \rightarrow c⁻x

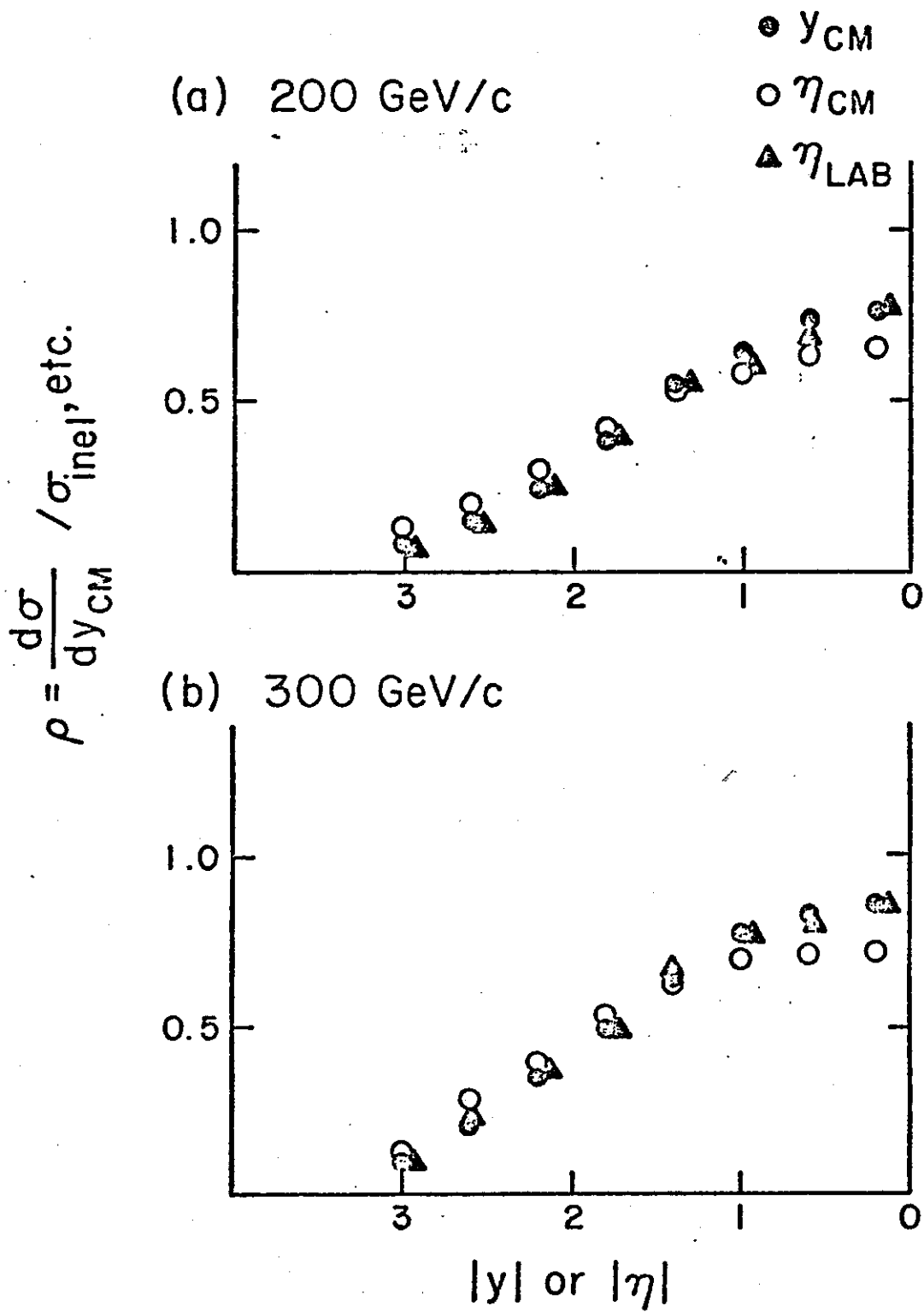
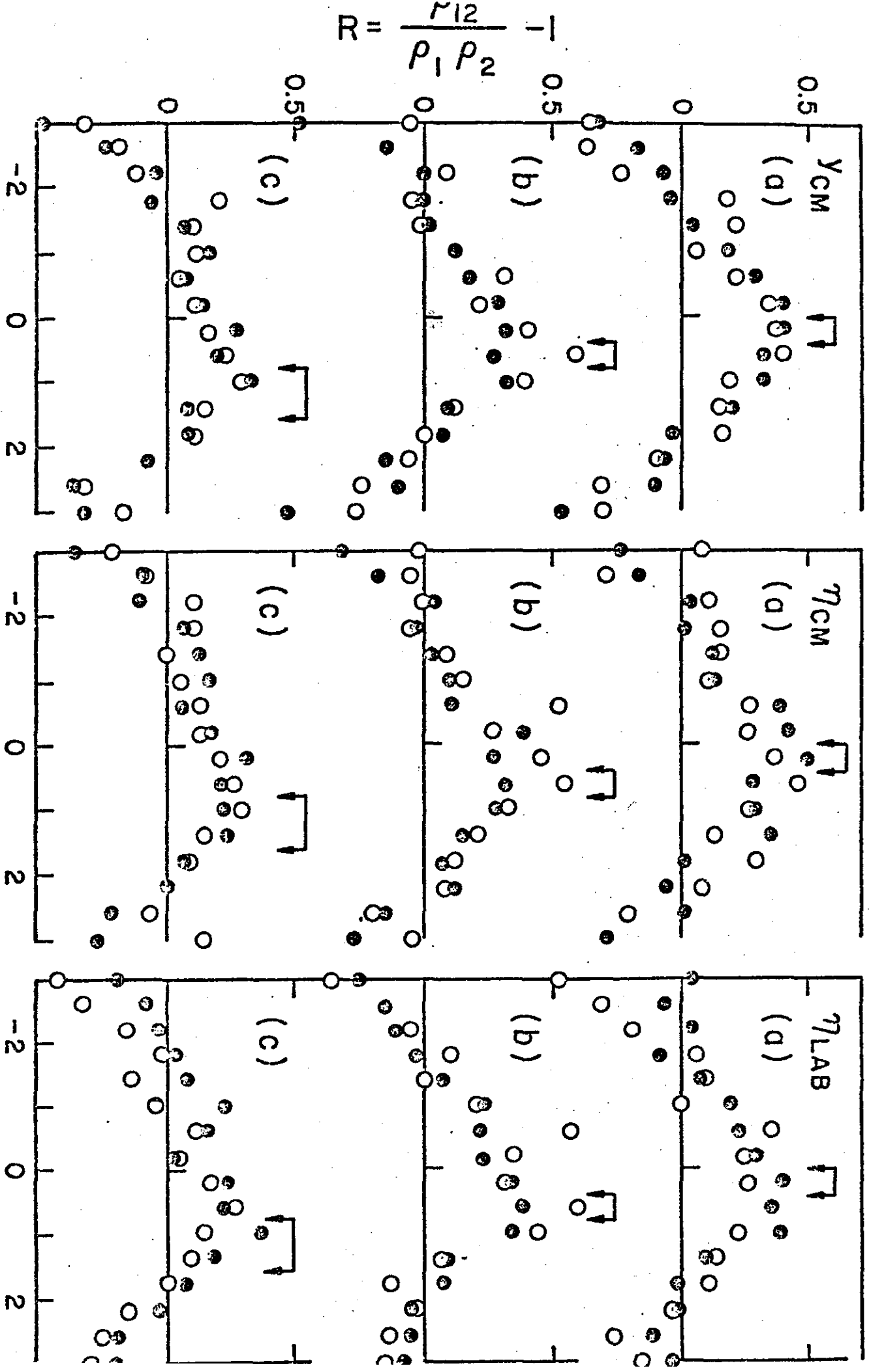


FIGURE 1

$$R = \frac{p_{12}(r_1, r_2)}{p_1(r_1)p_2(r_2)} - 1$$

- pp → c⁺c⁻x
- (a) 0 < r₂ < 0.4
 - (b) 0.4 < r₂ < 0.8
 - (c) 0.8 < r₂ < 1.6



$$r_1 = \eta_{-..}(1)$$

$$r_1 = \eta_{-..}(1)$$

$$r_1 = \eta_{-..}(1)$$

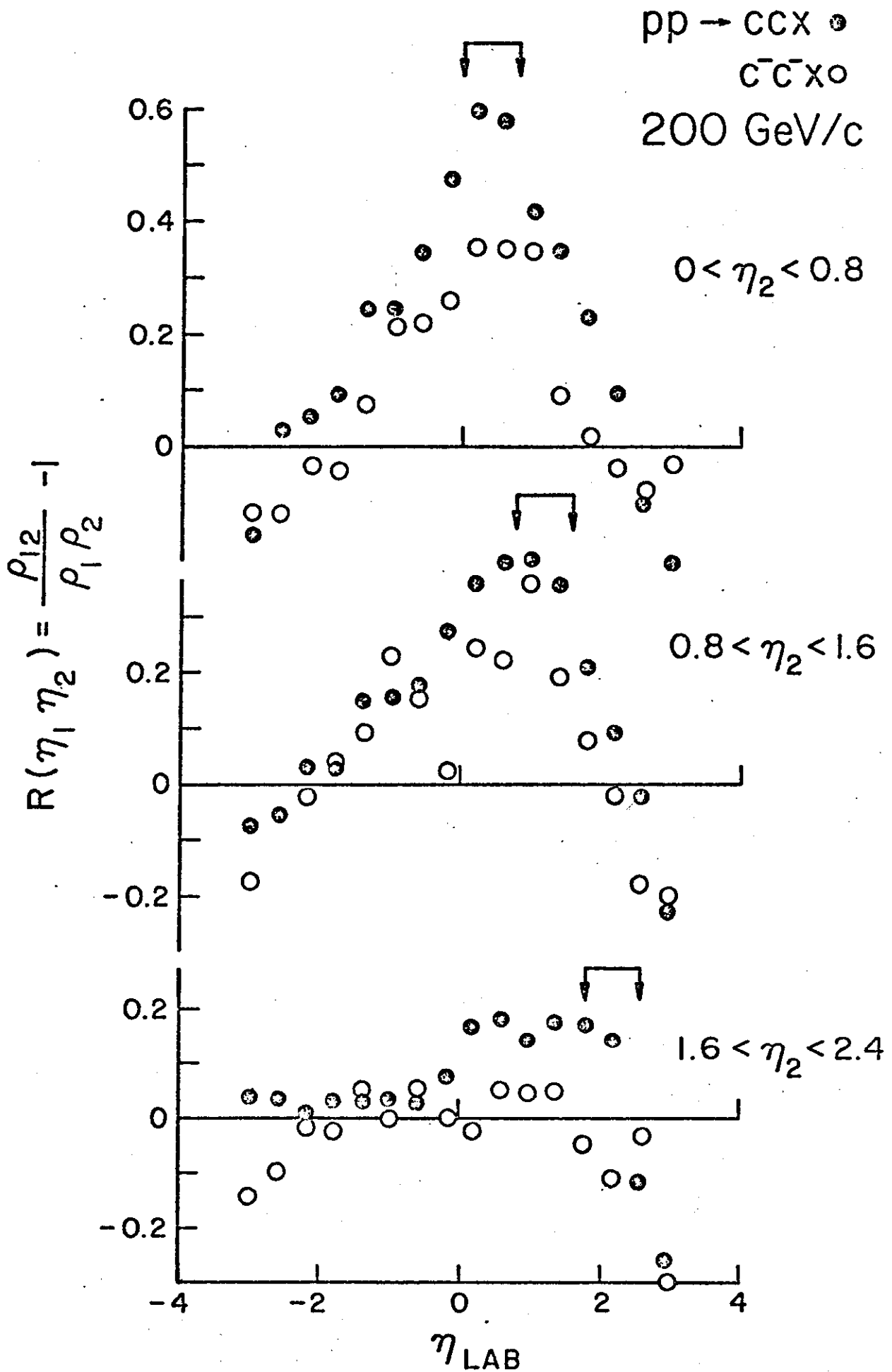


FIGURE 3